

# Quantitative Analysis of T Cell Receptor Complex Interaction Sites Using Genetically Encoded Photo-Cross-Linkers

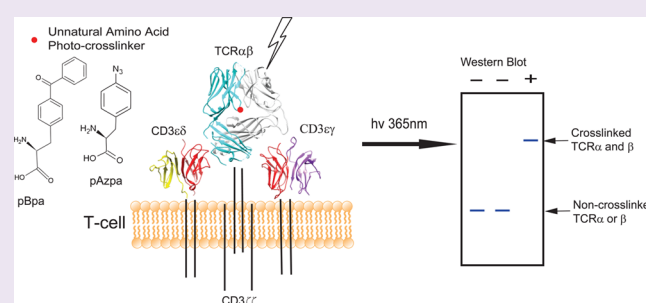
Wenjuan Wang,<sup>‡</sup> Tianqi Li,<sup>‡</sup> Klara Felsovalyi,<sup>§</sup> Chunlai Chen,<sup>||</sup> Timothy Cardozo,<sup>§</sup> and Michelle Krogsgaard<sup>\*,†,‡</sup>

<sup>†</sup>Department of Pathology, <sup>‡</sup>Laura and Isaac Perlmutter Cancer Center, and <sup>§</sup>Department of Biochemistry and Molecular Pharmacology New York University School of Medicine, New York, United States

<sup>||</sup>Pennsylvania Muscle Institute, Perelman School of Medicine, University of Pennsylvania, Philadelphia, Pennsylvania United States

## S Supporting Information

**ABSTRACT:** The T cell receptor (TCR)-cluster of differentiation 3 (CD3) signaling complex plays an important role in initiation of adaptive immune responses, but weak interactions have obstructed delineation of the individual TCR-CD3 subunit interactions during T cell signaling. Here, we demonstrate that unnatural amino acids (UAA) can be used to photo-cross-link subunits of TCR-CD3 on the cell surface. Incorporating UAA in mammalian cells is usually a low efficiency process. In addition, TCR-CD3 is composed of eight subunits and both TCR and CD3 chains are required for expression on the cell surface. Photo-cross-linking of UAAs for studying protein complexes such as TCR-CD3 is challenging due to the difficulty of transfecting and expressing multisubunit protein complexes in cells combined with the low efficiency of UAA incorporation. Here, we demonstrate that by systematic optimization, we can incorporate UAA in TCR-CD3 with high efficiency. Accordingly, the incorporated UAA can be used for site-specific photo-cross-linking experiments to pinpoint protein interaction sites, as well as to confirm interaction sites identified by X-ray crystallography. We systemically compared two different photo-cross-linkers—p-azido-phenylalanine (pAzpa) and H-p-Bz-Phe-OH (pBpa)—for their ability to map protein subunit interactions in the 2B4 TCR. pAzpa was found to have higher cross-linking efficiency, indicating that optimization of the selection of the most optimal cross-linker is important for correct identification of protein–protein interactions. This method is therefore suitable for studying interaction sites of large, dynamic heteromeric protein complexes associated with various cellular membrane systems.



T cells play a central role in adaptive immunity through regulation of responses by other immune cells or directly attacking infected or cancerous cells. The T cell receptor (TCR)-cluster of differentiation 3 (CD3) signaling complex is responsible for mediating specific CD4<sup>+</sup> and CD8<sup>+</sup> T cell responses to self- and foreign antigens.<sup>1</sup> TCR-CD3 is composed of disulfide-linked TCRαβ heterodimers and noncovalently associated CD3εδ, CD3εγ heterodimers, and CD3ζζ homodimers.<sup>2</sup> The complementarity determining regions (CDRs) of the TCRαβ variable regions are responsible for antigen–major histocompatibility complex (MHC) recognition,<sup>3</sup> while the long cytoplasmic tails of CD3 are vital in propagating the triggered TCR signal and interacting with the intracellular signaling machinery.<sup>4</sup> Therefore, expression of both TCR and CD3 chains is required on the cell surface to trigger T cell responses. In addition, TCRαβ has to be assembled into a complex with the CD3εδ, εγ, and ζζ dimers in order to reach the cell surface.<sup>5–8</sup> Thus, TCR-CD3 represents a multichain membrane signaling protein complex that is very challenging to study. Although biophysical and biochemical studies using soluble, purified proteins have provided a wealth of information on the structure and function of TCR-CD3,<sup>3,9</sup>

problems arise due to the transient and/or low-affinity interactions among the macromolecules, which are not maintained when the proteins are removed from their cellular context.<sup>5</sup> Furthermore, because TCR-CD3 is membrane-associated, the membrane environment regulates its structure, interactions, and function.<sup>10</sup> One strategy to circumvent these challenges is to incorporate photoactivatable unnatural amino acid (UAA) cross-linkers at specific sites in TCR-CD3 to covalently cross-link and capture the interactions among the signaling complex subunits as they occur in a native membrane environment. Here, we demonstrate the feasibility of this approach by incorporating UAAs into the TCR and cross-linking TCRα and β chains. This approach could be a powerful tool for investigating TCR and CD3 interactions to reveal T cell signaling mechanism in mammalian cells.

Incorporation of UAAs is a powerful method for studying protein–protein interactions. Different UAAs bearing unique side chains, such as benzophenone, aryl azide, and diazir-

**Received:** May 6, 2014

**Accepted:** July 25, 2014

**Published:** July 25, 2014

ine<sup>11–15</sup> can be genetically incorporated into proteins in live cells through reprogramming the genetic code.<sup>16</sup> Briefly, orthogonal tRNA-aminoacyl-tRNA synthetases (tRNA-aaRS), which are engineered to incorporate UAAs in response to unique codons, such as the amber stop codon TAG, are introduced into live cells. As a result, when UAAs are present in the tissue culture medium, the engineered tRNA-aaRS allows incorporation of UAA into the nascent protein by the ribosome at the TAG site. This approach provides a convenient way to site-specifically modify proteins with UAAs bearing unique side chains. Previously, UAAs have been genetically incorporated in *Escherichia coli*,<sup>17</sup> yeast,<sup>18,19</sup> and mammalian cells<sup>12,20–25</sup> using tRNA-aaRS pairs. However, the incorporation efficiency is generally low in mammalian cells.<sup>23</sup> Improving UAA incorporation efficiency by optimizing orthogonal tRNA-aaRS expression<sup>24–26</sup> or improving tRNA-aaRS affinity<sup>23</sup> has been pursued; however, the incorporation and application of UAAs in multisubunit signaling protein complexes such as TCR-CD3 has not been extensively examined.

Here, we report the successful genetic incorporation of the photoactivatable amino acids p-azido-phenylalanine (pAzpa) and H-p-Bz-Phe-OH (pBpa)<sup>25</sup> into the TCR $\alpha$  chain of TCR-CD3 in its native membrane environment in mammalian cells. We demonstrate that, after systematic optimization, UAA cross-linkers can be incorporated with high efficiency to probe specific interactions among a membrane protein complex such as TCR-CD3. We used the mouse 2B4 TCR,<sup>27</sup> and by incorporating the photo-cross-linkers into the TCR $\alpha$  chain, we were able to confirm specific interaction sites that were previously defined by X-ray crystallography.<sup>28</sup> Our result supports the hypothesis that this technique could potentially be widely used to probe interactions among complexes formed by weak interactions. In addition, as UAAs can be incorporated at specific protein sites, they can be used to pinpoint interaction sites between proteins that are difficult to assess by traditional methods of immunoprecipitation and cross-linking with nonspecific chemicals.

## RESULTS AND DISCUSSION

**Incorporation of Unnatural Amino Acids into the 2B4 TCR.** To test the feasibility of site-specific photo-cross-linking of TCR subunits, we used amber codon suppression to genetically incorporate UAAs with photo-cross-linking abilities into the previously biochemically and structurally well-characterized 2B4 TCR.<sup>28</sup> We used the X-ray crystal structure of 2B4 TCR (PDB: 3QJF)<sup>28</sup> (Figure 1a) to identify three amino acids (Arg39, Gly40, and Ser41) from the  $\alpha$  chain that are in close contact with the  $\beta$  chain. The shortest distances calculated between the chosen amino acids to nearest atoms on the  $\beta$  chain were 2.62, 3.92, and 3.68 Å for Arg39, Gly40, and Ser41, respectively (Supporting Information Table S1), and are generally thought to be within the distance needed for cross-linking.<sup>20</sup> A TAG stop codon was incorporated into the recombinant cDNA at the position encoding each amino acid. As a negative control we selected an amino acid, Lys65, that is distant from the TCR $\beta$  chain, such that cross-linking is not expected to occur. We compared two UAA photo-cross-linkers—pAzpa and pBpa (Figure 1b)—which have different sizes, photoreactive mechanisms, and cross-linking amino acid preferences.<sup>29,30</sup>

The selected amino acids were predicted to cross-link with varying degrees of efficiency (Arg39, Gly40, Ser41) or not to cross-link (Lys65). For those predicted to cross-link, we also

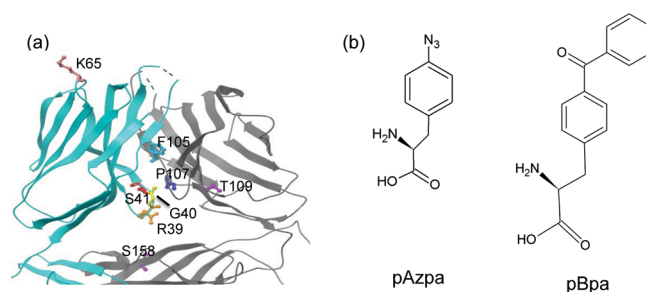


**Figure 1.** Structural illustration of 2B4 TCR and UAAs. (a) Ribbon diagram representation of the 2B4 TCR (PDB: 3QJF) with TCR $\alpha$  chain in cyan and TCR $\beta$  chain in gray. Residues mutated for UAA incorporation are Ser41 (red), Arg39 (orange), Gly40 (yellow), and Lys65 (pink). When calculating distance of the selected residues using center of mass of amino acids to main chain atoms of TCR $\beta$  chain, Ser41 shows the shortest distance to its interaction site Pro107 (dark blue). When considering UAA cross-linking preference, the closest pairs of residues are Ser41 (red) with Phe105 (light blue), Arg39 (orange) with S158 (purple), and Gly40 (yellow) with Thr109 (purple). (b) Structures of the UAA photo-cross-linkers pAzpa and pBpa.

calculated which TCR $\beta$  atoms fall into a 9–10 Å radius, indicating potential cross-linking partners (Supporting Information Table S2). Based on these measurements, all three selected residues have numerous potential cross-linking partners within an appropriate distance.

### U6 Promoter Increases UAA Incorporation Efficiency.

To optimize the incorporation of UAA into the 2B4 TCR, we analyzed the efficiency of different orthogonal amber suppressor tRNA-aminoacyl-tRNA synthetase (tRNA-aaRS) constructs, including PSWAN-pAzpa,<sup>25</sup> EAziRS,<sup>23</sup> PU6-pAzpa, and PU6-EAziRS for pAzpa incorporation; and PSWAN-pBpa,<sup>25</sup> EBzoRS,<sup>23</sup> PU6-pBpa, and PU6-EBzoRS for pBpa incorporation. The construction of PSWAN-pAzpa/pBpa (PSWAN plasmids), PU6-pAzpa/pBpa/EAziRS/EBzoRS (PU6 plasmids), and EAziRS/EBzoRS is illustrated in Figure 2a. The construction of PSWAN-pAzpa/pBpa has previously been described.<sup>25</sup> Briefly, the PSWAN plasmid has three copies of *B. stearothermophilus* tRNAs (BstRNA) and a mutant *E. coli* tyrosyl-tRNA synthetase (EcTyrRS). The BstRNA has naturally occurring internal A and B boxes recognized by RNA polymerase III in eukaryotes. The PU6 plasmid was modified from the PSWAN backbone with one copy of BstRNA and a human U6 small nuclear promoter (U6) added to improve the efficiency of expression of tRNAs. The EBzoRS and EAziRS plasmids include a pol III promoter H1,<sup>23,31</sup> EcTyrRS, and EcTyrRS.<sup>20</sup> The orthogonal tRNA-aaRS plasmids were cotransfected with the PSWAN-GFP37TAG<sup>25</sup> plasmid, which has an amber stop mutation at position Tyr37 of GFP, into Human Embryonic Kidney (HEK) 293 T cells followed by addition of the UAAs pAzpa and pBpa to the tissue culture medium. GFP expression was quantified 48 h after transfection using flow cytometry to directly compare the efficiency of UAA incorporation. We observed that PU6-pAzpa and PU6-EAziRS had significantly higher expression of GFP than PSWAN-pAzpa and EAziRS with pAzpa incorporation (Figure 2b), which suggested that the U6 promoter in the PU6-pAzpa or PU6-EAziRS constructs may play an important role in promoting tRNA expression, subsequently enhancing the UAA incorporation efficiency. Similarly, we observed that PU6-pBpa and PU6-EBzoRS had higher expression of GFP than PSWAN-

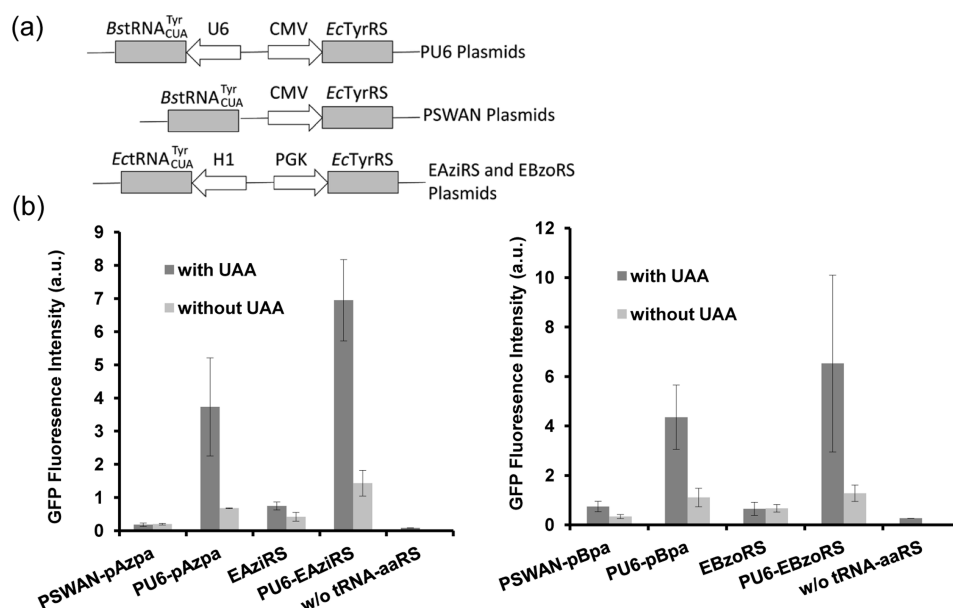


**Figure 2.** U6 promoter increases UAA incorporation efficiency. (a) Schematic illustration of different tRNA-aaRS expression plasmids. The PSWAN plasmid (PSWAN\_pAzpa/pBpa) has three copies of *B. stearothermophilus* tRNAs (BstRNA) and a mutant *E. coli* tyrosyl-tRNA synthetase (EcTyrRS). The BstRNA has naturally occurring internal A and B boxes recognized by the RNA polymerase III in eukaryotes. The PU6 (PU6\_pAzpa/pBpa/EBzoRS/EAziRS) plasmid has one copy of BstRNA and a human U6 small nuclear promoter (U6) added to improve the efficiency of expression of tRNAs. The EBzoRS and EAziRS plasmids include a pol III promoter H1,<sup>23,31</sup> EctRNA, and EcTyrRS.<sup>20</sup> (b) Total GFP intensity with pAzpa (left) and pBpa (right) incorporation after transfection of tRNA-aaRS and PSWAN-GFP37TAG plasmids to HEK293 T cells. GFP fluorescence intensity was quantified by flow cytometry. Error bars represent Standard Error of the Mean (SEM);  $n = 3$  a.u. represents arbitrary unit.

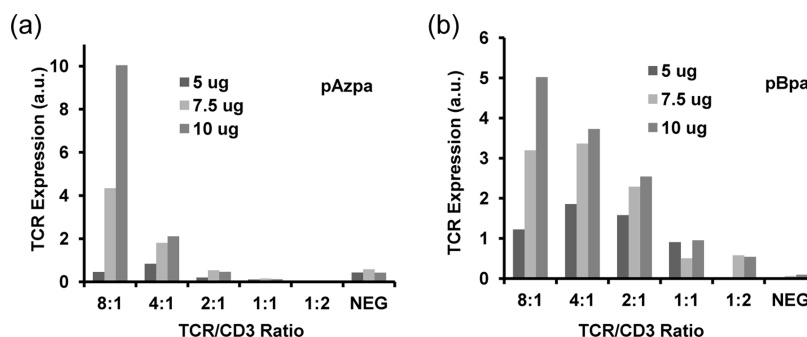


**Figure 3.** Efficient incorporation of UAA into the 2B4 TCR/CD3 signaling complex. Influence of TCR/CD3 ratio and transfection amount for TCR surface expression when using pAzpa (a) versus pBpa (b) for incorporation. We transfected 2.5  $\mu$ g, 5  $\mu$ g or 7.5  $\mu$ g of TCR and CD3 plasmid DNA into HEK293 T cells. We also varied the ratio of TCR/CD3 plasmid DNA from 8:1, 4:1, 2:1, and 1:1. TCR expression was quantified by PE-conjugated anti-TCR V $\beta$ 3 staining followed by flow cytometry analysis.

pBpa and EBzoRS with pBpa incorporation. Importantly, PSWAN-GFP37TAG contains not only the GFP reporter but also three copies of a cassette expressing BstRNA and therefore contributes to a background of tRNA cassette in our experiments. Therefore, the quantification of the precise fold increase that is contributed by the promoter cannot be calculated due to this general background. However, our data shows that PU6 plasmids are the most efficient.

**Efficient Incorporation of UAA in the 2B4 TCR/CD3 Signaling Complex.** The TCR-CD3 signaling complex is composed of the disulfide-linked TCR $\alpha\beta$  heterodimer and the noncovalently associated CD3 $\epsilon\delta$ ,  $\epsilon\gamma$ , and  $\zeta\xi$  chains, all of which are required for efficient expression at the cell surface.<sup>32,33</sup> The difficulty of transfecting and expressing multiple subunits of TCR-CD3, combined with generally low UAA incorporation efficiency in mammalian cells is a major technical barrier to the use of UAA incorporation in studying the TCR-CD3 complex.

To facilitate stoichiometric expression of different subunits, self-cleavable 2A peptide linkers were used to connect TCR $\alpha$  and  $\beta$  chains or CD3 $\delta$ ,  $\epsilon$ ,  $\gamma$ , and  $\xi$  chains.<sup>34</sup> Subsequently, constructs containing TCR and CD3 were cotransfected with tRNA-aaRS constructs into HEK293 T cells. We investigated how the ratio and total amount of TCR/CD3 DNA influences the surface expression of TCR after UAA incorporation. We cotransfected 2.5  $\mu$ g of tRNA-aaRS plasmid DNA with 2.5  $\mu$ g, 5  $\mu$ g or 7.5  $\mu$ g of TCR and CD3 plasmid DNA into HEK293 T cells. We also varied the ratio of TCR:CD3 from 8:1, 4:1, 2:1, and 1:1 (Figure 3). TCR expression was quantified by flow cytometry. We found that 7.5  $\mu$ g of TCR and CD3 total plasmid DNA is optimal for transfection and that 8:1 weight ratio of TCR/CD3 has the highest TCR expression (around 100-fold increase compared to the lowest TCR expression) (Figure 3).

**Optimization of Photo-Cross-Linking Time Is Important for Efficient UAA Incorporation.** After incorporation of



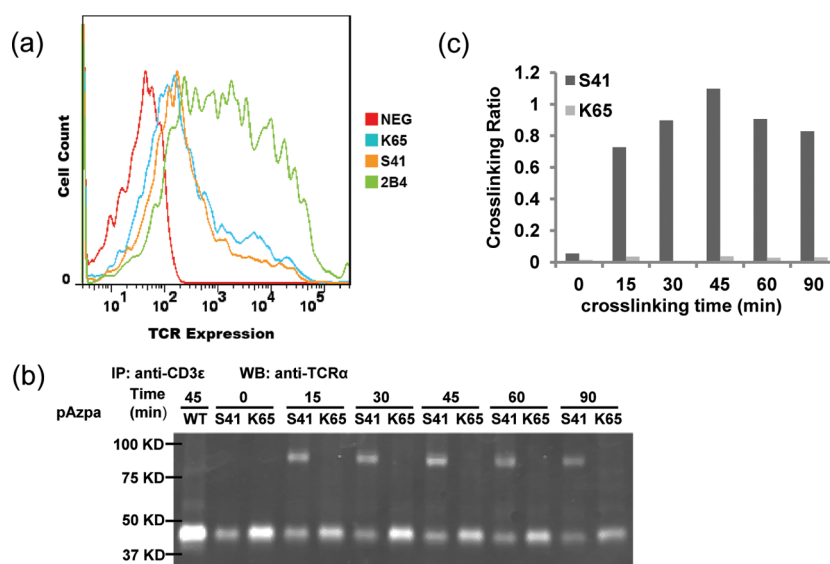


**Figure 4.** In-cell surface protein photo-cross-linking. (a) TCRs were expressed on the cell surface at lower levels than WT after pAzpa incorporation. Two amino acids Ser41 and Lys65 (non-cross-linking control) on TCR $\alpha$  were mutated to incorporate UAA. TCR expression was quantified by PE-conjugated anti-TCR V $\beta$ 3 staining followed by flow cytometry analysis. (b) Cells expressing TCRs with pAzpa incorporated were cross-linked under 365 nm UV light for 0 min, 15 min, 30 min, 45 min, 60 min, or 90 min. Then, cells were lysed, and TCR-CD3 complexes were immunoprecipitated with biotin anti-CD3 $\epsilon$  and probed with anti-TCR $\alpha$  antibody using Western blot. Lower bands between 37 and 50 kD represent non-cross-linked TCR $\alpha$  chain and upper bands between 75 and 100 kD represent cross-linked TCR $\alpha$  and  $\beta$  chains. (c) Quantification of cross-linking efficiency at different cross-linking incubation times. We quantify the cross-linked complex band and non-cross-linked bands from Western blot image. Cross-linking efficiency was calculated using the ratio of cross-linked compound intensity to non-cross-linked TCR intensity from Western blot image.

pAzpa or pBpa into the TCR, photo-cross-linking was performed for varied lengths of time (0, 15, 30, 45, 60, 90 min) to identify the UV-exposure time to obtain maximum photo-cross-linking efficiency of TCR $\alpha$  and  $\beta$  chains. After in-cell photo-cross-linking using UV at 365 nm, TCR-CD3 complex was precipitated using biotin-labeled anti-CD3 $\epsilon$ <sup>35</sup> antibody, followed by purification with streptavidin beads. After purification, the subunits were separated in the presence of a reducing agent by SDS-PAGE, followed by Western blot analysis to detect individual TCR subunits and cross-linked complexes. To facilitate Western blot detection of TCR $\beta$  chain, a V5 epitope tag was introduced after the TCR $\beta$  chain so that the presence of TCR $\beta$  in the cross-linked complex could be directly detected using an anti-V5 antibody. The expression of the wild type 2B4 TCR, 2B4 TCR with the Ser41 mutation, and negative control 2B4 TCR with the Lys65 mutation on the  $\alpha$  chain is shown in Figure 4a. The expression levels of the Ser41 and Lys65 mutants were similar and were both lower than wild-type 2B4 TCR. To determine cross-linking efficiency, the blots were probed with anti-TCR $\alpha$  Va11.1 antibody and anti-V5 antibodies. Cross-linking efficiency was quantified using the ratio of cross-linked compound intensity to non-cross-linked TCR intensity (Figure 4b). Non-cross-linked TCR $\alpha$  and  $\beta$  chains migrate at apparent molecular masses between 37 and 50 kDa, and cross-linked TCR $\alpha$  and  $\beta$  chains migrate at apparent molecular masses between 75 and 100 kDa (Figure 4b and Supporting Information Figure 1). pAzpa efficiently cross-linked TCR $\alpha$  and  $\beta$  chains in 15 min, and its efficiency increased when cross-linking time was increased up to 45 min (Figure 4c). Longer cross-linking times, however, did not increase photo-cross-linking efficiency (Figure 4c). Cross-linking with pBpa produced similar results. Overall, cross-linking times between 15 and 45 min are favorable for both cross-linkers.

#### pAzpa is More Efficient at Photo-Cross-Linking TCR $\alpha$ and $\beta$ Chains Compared with pBpa.

To further investigate the specificity of the in-cell photo-cross-linking approach and to compare pAzpa and pBpa photo-cross-linking efficiency, we performed cross-linking experiments for TCR $\alpha$  and  $\beta$  chains using pAzpa and pBpa. We quantified TCR and CD3 expression by flow cytometry using anti-TCR $\beta$  and anti-CD3 $\epsilon$  antibodies 48h post-transfection of HEK293 T cells. TCR with pAzpa (Figure 5a) or pBpa (Figure 5b) incorporated at Arg39, Gly40, Ser41, and Lys65 were expressed on the cell surface at comparable levels. Expression of TCR with incorporation of pAzpa was lower than wild type 2B4 TCR (Figure 5a), while expression of TCR with incorporation of pBpa was comparable to wild type levels (Figure 5b). However, in both cases CD3 was well expressed on the cell surface, which suggests that the incorporation of UAA in the 2B4 TCR has limited influence on CD3 expression and does not interfere with TCR interactions with CD3. After photo-cross-linking for 30 min, TCR cross-linking efficiency was evaluated by immunoprecipitation and Western blot analysis (Figure 5c and d). Cross-linked TCR $\alpha$  and  $\beta$  chains were visualized by colocalization of anti-TCR $\alpha$  and anti-V5 antibodies (Figure 5c and d). Consistent with the X-ray crystallography data, the pAzpa and pBpa showed functional cross-linking when incorporated at positions Arg39, Gly40, and Ser41, but not at the control Lys65 position (Figure 5c and d), demonstrating the specificity of cross-linking. In all, when comparing the cross-linking efficiency of pAzpa and pBpa through the relative intensities of the bands corresponding to the cross-linked product (Figure 5e), pAzpa exhibited higher cross-linking efficiency than pBpa at the specific cross-linking sites chosen in our study.

The use of UAAs to study the interactions of membrane protein complexes such as the TCR signaling complex is challenging due to inefficient UAA incorporation and low

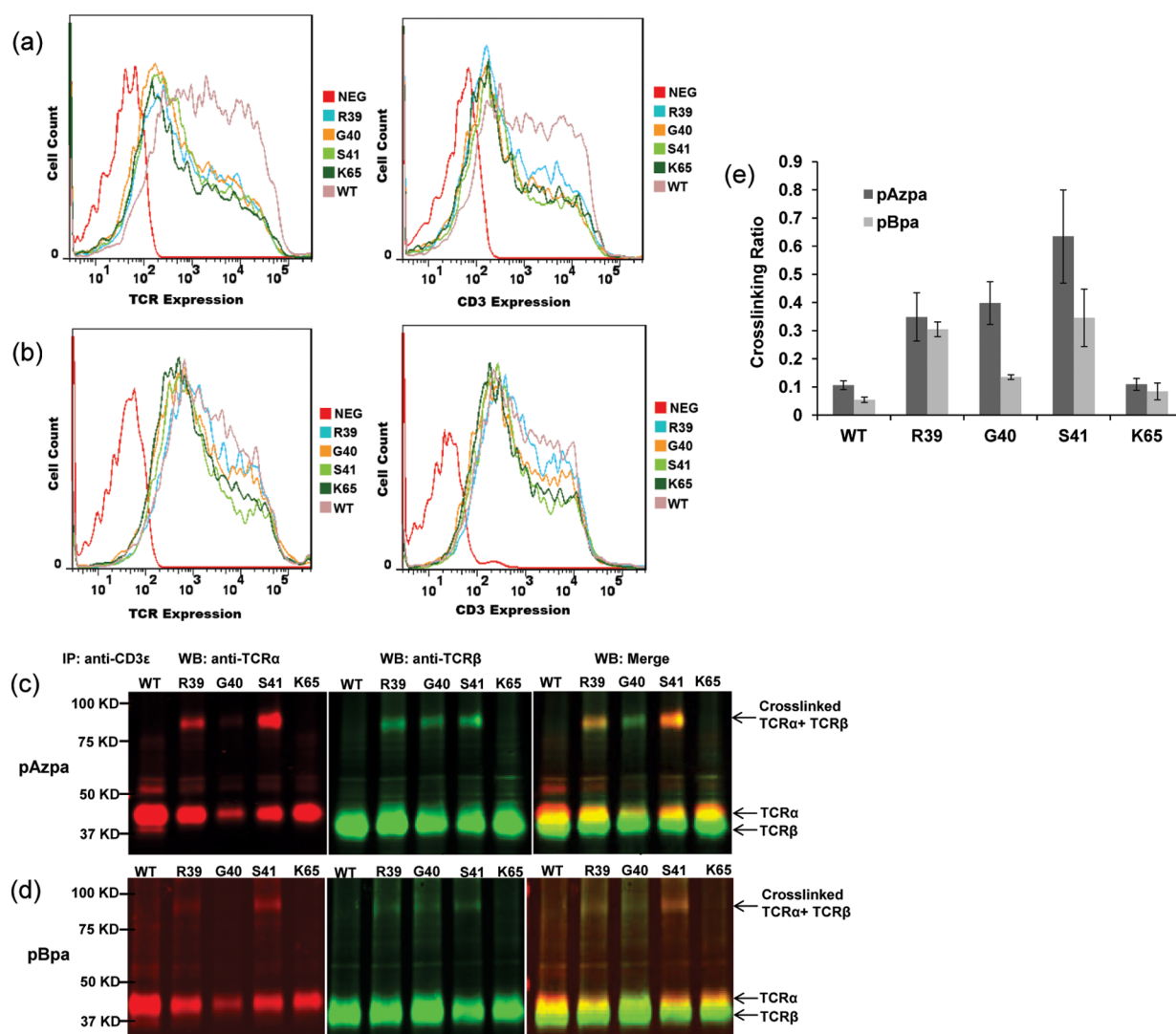


**Figure 5.** pAzpa is more efficient in cross-linking TCR subunits than pBpa. TCR and CD3 expression with (a) pAzpa and (b) pBpa incorporated on different sites of the TCR $\alpha$  chain. TCR and CD3 expression was quantified by PE-conjugated anti-TCR V $\beta$ 3 and APC-conjugated anti-CD3 $\epsilon$  (145-2C11) staining followed by flow cytometry analysis. Photo-cross-linking of TCR $\alpha$  and  $\beta$  chains with (c) pAzpa and (d) pBpa as photo-cross-linkers. Cells expressing TCRs with pAzpa or pBpa incorporated were cross-linked by UV light (365 nm) for 30 min. Immunoprecipitation with biotin anti-CD3 $\epsilon$  followed by Western blotting using anti-TCR $\alpha$  and anti-V5 antibodies were performed after UV-cross-linking. Lower bands between 37 and 50 KD represent non-cross-linked TCR $\alpha$  or  $\beta$  chain and upper bands between 75 and 100 KD represent cross-linked TCR $\alpha$  and  $\beta$  chains. Wild type 2B4 TCR and Lys65 are used as non-cross-linking control. (e) Quantification of cross-linking efficiency calculated from cross-linked and non-cross-linked band from Western blot image. Error bars represents SEM,  $n = 2$ . (c) Quantification of cross-linking efficiency at different cross-linking incubation times. We quantify the cross-linked complex band and non-cross-linked bands from Western blot image. Cross-linking efficiency was calculated using the ratio of cross-linked compound intensity to non-cross-linked TCR intensity from Western blot image.

protein yields. In our study, we found that driving tRNA expression by a human U6 small nuclear promoter (U6) can significantly increase UAA incorporation efficiency. This result is supported by previous studies that showed that the U6 promoter, which successfully expresses short interfering RNAs in mammalian cells, can greatly promote the expression of orthogonal *E. coli* tRNA in mammalian cells and is more efficient than the human H1 promoter (H1).<sup>24,36</sup> In addition, the U6 promoter has previously been used to increase tRNA expression for the successful application of UAAs in studying G protein-coupled receptors and their binding path.<sup>37</sup> Our system for incorporating UAAs in TCR-CD3 complexes includes three plasmids encoding tRNA-aaRS, TCR, and CD3. We increased the amount of plasmid DNA to improve transfection efficiency, and we optimized the TCR/CD3 plasmid DNA ratio to ensure

optimal expression of both TCR and CD3. Together, these approaches resulted in high UAA incorporation efficiency in TCR-CD3.

pBpa<sup>12,25</sup> is generally used in photo-cross-linking, with few examples using pAzpa.<sup>38</sup> Benzophenones (pBpa) are activated by relatively long wavelength light (350–365 nm)<sup>29</sup> compared to aryl azides (pAzpa) (<330 nm).<sup>39</sup> Therefore, pBpa would be expected to minimize the incidence of nonspecific cross-linking and nucleic acid damage. However, we found that pAzpa can be efficiently photoactivated at the longer wavelength of 365 nm when incorporated into proteins, and we obtained higher cross-linking efficiency with pAzpa than pBpa. The reasons for this might be the following: first, benzophenone is more selective, exhibiting a strong preference to react with methionine;<sup>29</sup> the cross-linking efficiency might be influenced by this preference.

Second, benzophenone is bigger than aryl azides, making it more susceptible to geometric constraints when reacting with other residues. Thus, the smaller size of aryl azides may be advantageous in protein interactions that are more sensitive to perturbations. Generally, we obtained more efficient cross-linking when using pAzpa. However, as the previous literature has shown that different results with pAzpa and pBpa can be obtained when incorporated at different positions and under different experimental conditions,<sup>38</sup> comparing the two cross-linkers for each individual protein under specific experimental conditions might be optimal.

In all, we have successfully incorporated UAAs into a TCR-CD3 membrane protein complex, and our results demonstrate the feasibility of this method in studying TCR subunit interactions by photo-cross-linking. This technique can be useful in studying complex protein interactions, since theoretically, the UAA photo-cross-linker can be site-specifically incorporated at any site of a protein. In our study, we utilized this technique to identify the interaction sites between two protein subunits, which verify the interaction sites identified by crystallography. In addition, the results can be taken as evidence that the structure resolved in the crystal corresponds at least partly to the “real” structure in its native environment, although a more extensive cross-linking study would be needed to confirm this. In addition, this technique can be used to capture protein interactions at various stages in the signal transduction process, since the photo-cross-linker can be excited at relevant time-scales.

## METHODS

**Plasmid Construction.** The PSWAN-pAzpa, PSWAN-pBpa,<sup>25</sup> and PU6-pBpa plasmids were generous gifts from Dr. Peter G. Schultz at the Scripps Research Institute. The EBzoRS and EAziRS plasmids<sup>23</sup> were generous gifts from Dr. Lei Wang at the Salk Institute for Biological Studies. We replaced cDNA encoding the tRNA synthetase for recognition of pBpa in PU6-pBpa plasmid with tRNA synthetase in PSWAN-pAzpa,<sup>25</sup> EAziRS, and EBzoRS<sup>23</sup> to create PU6-pAzpa, PU6-EaziRS, and PU6-EBzoRS. cDNA encoding 2B4 TCR $\alpha$  and  $\beta$  chains<sup>14,15,40</sup> was subcloned into the pcDNA3.1/Zeo (+) vector (Life Technologies) using NotI and XhoI restriction enzymes. Similarly, cDNAs encoding mouse CD3 $\delta$ , CD3 $\epsilon$ , and CD3 $\gamma$  chains were subcloned into the pcDNA3.1/Zeo (+) vector using NotI and EcoRI restriction enzymes. Self-cleavable 2A peptides were introduced for optimal TCR and CD3 expression, as previously described.<sup>34</sup> A V5 epitope tag was added to the C-terminus of TCR $\beta$  for the detection of TCR $\beta$  in Western blot analysis. Site-specific amber stop codons (TAG), used to facilitate nonspecific amino acid incorporation, were introduced into 2B4 TCR sequence using the QuikChange Site-Directed Mutagenesis Kit (Stratagene).

**Expression of 2B4 TCR with UAA Mutants in Mammalian Cells.** HEK293 T cells were transfected with three plasmids expressing tRNA-aaRS, 2B4 TCR, and CD3 $\epsilon\delta$ ,  $\epsilon\gamma$ ,  $\zeta\zeta$  using the Xfect Transfection Reagent (Clontech). The day before transfection, 0.5 million cells were plated in a well of a 6-well cell culture plate to obtain approximately 60% confluence at the time of transfection. For transfection, Xfect polymer was mixed with plasmids and added to the cell culture medium. After a 4 h incubation at 37 °C in 5% CO<sub>2</sub>, the transfection reagent mixture was replaced with DMEM medium containing 1 mM of either 4-azido-L-phenylalanine (pAzpa) (Chem-Impex International) or H-p-Bz-Phe-OH (pBpa) (Bachem). Cells were used for photo-cross-linking experiments 48 h post-transfection to allow expression of TCR and CD3 molecules on the cell surface.

**Flow Cytometry Analysis.** Cells were collected 48 h post-transfection and stained with PE-conjugated anti-TCR V $\beta$ 3 (BD Pharmingen) and APC-conjugated anti-CD3 $\epsilon$  (145-2C11) (BD Pharmingen) in FACS Buffer (PBS, 2% (v/v) FBS, 0.1% (w/v)

sodium azide) for 30 min. Subsequently, the samples were run on BD LSRII and data was analyzed by Flowjo 7.6 (TreeStar) for expression of TCR and CD3 proteins.

**Photo-Cross-Linking, Surface Immunoprecipitation and Western Blots.** To photo-cross-link TCR $\alpha$  and  $\beta$  chains, cells were first transfected with the appropriate plasmid mixtures, then collected and plated in 6-well tissue culture plates (BD Biosciences) and finally photo-cross-linked by exposing the cells to 365 nm UV-light using a UVP CL-1000 ultraviolet cross-linker instrument for different times as outlined in individual experiments. After photo-cross-linking, cells were treated with 25  $\mu$ g/mL CD16/CD32 (BD Pharmingen) for 30 min, followed by treatment with 25  $\mu$ g/mL H57 (BD Pharmingen) for 30 min. Next, 25  $\mu$ g/mL biotinylated mouse anti-CD3 $\epsilon$  (145-2C11) (eBioscience) was added for 30 min. Cells were washed between each treatment after photo-cross-linking with ice-cold HBSS (Hank's balanced salt solution) /2% (v/v) FBS/0.05% (m/v) sodium azide. Afterward, cells were lysed in TBS (Tris-buffered saline) (pH 8.0) /1% (v/v) IGEPAL-CA630 (Sigma) containing 1X Complete protease inhibitors (Roche) for 30 min. The TCR/CD3 complex was purified by adding Dynabeads M-280 Streptavidin (Life Technologies) to the lysis supernatant. The beads were boiled in PBS, 0.1% (m/v) SDS with SDS-PAGE reducing buffer with  $\beta$ -mercaptoethanol (Boston Bio-Products). TCR-CD3 complexes were resolved by SDS-PAGE gel and transferred to nitrocellulose membrane (Life Technologies). In subsequent Western blot analysis, membranes were first probed with an anti-TCR Va11.1 antibody (BD Biosciences) and a rabbit anti-V5 antibody (Genscript), followed by corresponding secondary antibodies—IRDye 680LT-conjugated donkey anti-mouse IgG (H + L) or IRDye 800CW-conjugated donkey anti-goat IgG (H + L) (LI-COR Biosciences). Images were collected using Odyssey machine (LI-COR Biosciences) and analyzed using ImageJ or Image Studio Lite (LI-COR Biosciences). To quantify cross-linking efficiency based on Western blot, Image Studio Lite (LI-COR Biosciences) was used to quantify the intensity of the cross-linked protein bands and non-cross-linked protein bands. Subsequently, the ratio of cross-linked to non-cross-linked bands was calculated to obtain the cross-linking efficiency.

## ASSOCIATED CONTENT

### Supporting Information

This material is available free of charge via the Internet at <http://pubs.acs.org>.

## AUTHOR INFORMATION

### Corresponding Author

\*Email: [Michelle.Krogsgaard@nyumc.org](mailto:Michelle.Krogsgaard@nyumc.org).

### Notes

The authors declare no competing financial interest.

## ACKNOWLEDGMENTS

We thank NYU flow cytometry core for technical assistance and K. Malecek, D. Moogk, and A. Natarajan for helpful discussions and critical reading of the manuscript. We also thank T. P. Sakmar, S. Naganathan, and H. Tian from the Rockefeller University for technical advice and discussion. This work was supported by Laura and Isaac Perlmutter Cancer Center and The Interdisciplinary Melanoma Cooperative Group (IMCG) at New York University (NYU) Langone Medical Center, National Institutes of Health (NIH) grants from the National Institute of General Medical Sciences (NIGMS), 5R01GM85586 (to M.K.), and from the Office of the Director (OD), 4DP2OD004631 (to T.C.), and a Pew Scholar in Biomedical Sciences grant supported by the Pew Trust (to M.K.). Use of flow cytometry was sponsored from NYUCI Center Support Grant, NIH/NCI 5 P30CA16087-31.



## REFERENCES

- (1) Davis, M. M., Krogsgaard, M., Huppa, J. B., Sumen, C., Purbhoo, M. A., Irvine, D. J., Wu, L. C., and Ehrlich, L. (2003) Dynamics of cell surface molecules during T cell recognition. *Annu. Rev. Biochem.* 72, 717–742.
- (2) Call, M. E., Pyrdol, J., Wiedmann, M., and Wucherpfennig, K. W. (2002) The organizing principle in the formation of the T cell receptor–CD3 complex. *Cell* 111, 967–979.
- (3) Rudolph, M. G., Stanfield, R. L., and Wilson, I. A. (2006) How TCRs bind MHCs, peptides, and coreceptors. *Annu. Rev. Immunol.* 24, 419–466.
- (4) Kane, L. P., Lin, J., and Weiss, A. (2000) Signal transduction by the TCR for antigen. *Curr. Opin. Immunol.* 12, 242–249.
- (5) Call, M. E., and Wucherpfennig, K. W. (2005) The T cell receptor: Critical role of the membrane environment in receptor assembly and function. *Annu. Rev. Immunol.* 23, 101–125.
- (6) Delgado, P., and Alarcon, B. (2005) An orderly inactivation of intracellular retention signals control surface expression of the T cell antigen receptor. *J. Exp. Med.* 201, 555–566.
- (7) Wegener, A. M. K., Hou, X. H., Dietrich, J., and Geisler, C. (1995) Distinct domains of the Cd3- $\gamma$  chain are involved in surface expression and function of the T-Cell antigen receptor. *J. Biol. Chem.* 270, 4675–4680.
- (8) Morley, B. J., Chin, K. N., Newton, M. E., and Weiss, A. (1988) The lysine residue in the membrane-spanning domain of the  $\beta$ -chain is necessary for cell-surface expression of the T-cell antigen receptor. *J. Exp. Med.* 168, 1971–1978.
- (9) Wang, J. H., and Reinherz, E. L. (2012) The structural basis of  $\alpha\beta$  T-lineage immune recognition: TCR docking topologies, mechanotransduction, and co-receptor function. *Immunol. Rev.* 250, 102–119.
- (10) Huang, J., Meyer, C., and Zhu, C. (2012) T cell antigen recognition at the cell membrane. *Mol. Immunol.* 52, 155–164.
- (11) Kim, C. H., Axup, J. Y., and Schultz, P. G. (2013) Protein conjugation with genetically encoded unnatural amino acids. *Curr. Opin. Chem. Biol.* 17, 412–419.
- (12) Hino, N., Okazaki, Y., Kobayashi, T., Hayashi, A., Sakamoto, K., and Yokoyama, S. (2005) Protein photo-cross-linking in mammalian cells by site-specific incorporation of a photoreactive amino acid. *Nat. Methods* 2, 201–206.
- (13) Song, W., Wang, Y., Qu, J., and Lin, Q. (2008) Selective functionalization of a genetically encoded alkene-containing protein via “photoclick chemistry” in bacterial cells. *J. Am. Chem. Soc.* 130, 9654–9655.
- (14) Ai, H. W. (2012) Biochemical analysis with the expanded genetic lexicon. *Anal. Bioanal. Chem.* 403, 2089–2102.
- (15) Hao, Z., Hong, S., Chen, X., and Chen, P. R. (2011) Introducing bioorthogonal functionalities into proteins in living cells. *Acc. Chem. Res.* 44, 742–751.
- (16) Tanaka, Y., Bond, M. R., and Kohler, J. J. (2008) Photo-crosslinkers illuminate interactions in living cells. *Mol. Biosyst.* 4, 473–480.
- (17) Farrelly, I. S., Toroney, R., Hazen, J. L., Mehl, R. A., and Chin, J. W. (2005) Photo-cross-linking interacting proteins with a genetically encoded benzophenone. *Nat. Methods* 2, 377–384.
- (18) Chen, S., Schultz, P. G., and Brock, A. (2007) An improved system for the generation and analysis of mutant proteins containing unnatural amino acids in *Saccharomyces cerevisiae*. *J. Mol. Biol.* 371, 112–122.
- (19) Chin, J. W., Cropp, T. A., Anderson, J. C., Mukherji, M., Zhang, Z. W., and Schultz, P. G. (2003) An expanded eukaryotic genetic code. *Science* 301, 964–967.
- (20) Grunbeck, A., Huber, T., Sachdev, P., and Sakmar, T. P. (2011) Mapping the Ligand-Binding Site on a G Protein-Coupled Receptor (GPCR) Using Genetically Encoded Photocrosslinkers. *Biochemistry-U S* 50, 3411–3413.
- (21) Hino, N., Hayashi, A., Sakamoto, K., and Yokoyama, S. (2006) Site-specific incorporation of non-natural amino acids into proteins in mammalian cells with an expanded genetic code. *Nat. Protoc.* 1, 2957–2962.
- (22) Coin, I., Perrin, M. H., Vale, W. W., and Wang, L. (2011) Photo-cross-linkers incorporated into G-protein-coupled receptors in mammalian cells: A ligand comparison. *Angew. Chem., Int. Ed.* 50, 8077–8081.
- (23) Takimoto, J. K., Adams, K. L., Xiang, Z., and Wang, L. (2009) Improving orthogonal tRNA-synthetase recognition for efficient unnatural amino acid incorporation and application in mammalian cells. *Mol. Biosyst.* 5, 931–934.
- (24) Wang, W. Y., Takimoto, J. K., Louie, G. V., Baiga, T. J., Noel, J. P., Lee, K. F., Slesinger, P. A., and Wang, L. (2007) Genetically encoding unnatural amino acids for cellular and neuronal studies. *Nat. Neurosci.* 10, 1063–1072.
- (25) Liu, W. S., Brock, A., Chen, S., Chen, S. B., and Schultz, P. G. (2007) Genetic incorporation of unnatural amino acids into proteins in mammalian cells. *Nat. Methods* 4, 239–244.
- (26) Wang, Q., and Wang, L. (2008) New methods enabling efficient incorporation of unnatural amino acids in yeast. *J. Am. Chem. Soc.* 130, 6066–6067.
- (27) Hedrick, S. M., Matis, L. A., Hecht, T. T., Samelson, L. E., Longo, D. L., Heber-Katz, E., and Schwartz, R. H. (1982) The fine specificity of antigen and Ia determinant recognition by T cell hybridoma clones specific for pigeon cytochrome c. *Cell* 30, 141–152.
- (28) Newell, E. W., Ely, L. K., Kruse, A. C., Reay, P. A., Rodriguez, S. N., Lin, A. E., Kuhns, M. S., Garcia, K. C., and Davis, M. M. (2011) Structural basis of specificity and cross-reactivity in T cell receptors specific for cytochrome c-I-E-k. *J. Immunol.* 186, 5823–5832.
- (29) Dorman, G., and Prestwich, G. D. (1994) Benzophenone photophores in biochemistry. *Biochemistry U.S.* 33, 5661–5673.
- (30) Gritsan, N. P., Gudmundsdottir, A. D., Tigelaar, D., Zhu, Z. D., Karney, W. L., Hadad, C. M., and Platz, M. S. (2001) A laser flash photolysis and quantum chemical study of the fluorinated derivatives of singlet phenylnitrene. *J. Am. Chem. Soc.* 123, 1951–1962.
- (31) Myslinski, E., Ame, J. C., Krol, A., and Carbon, P. (2001) An unusually compact external promoter for RNA polymerase III transcription of the human H1RNA gene. *Nucleic Acids Res.* 29, 2502–2509.
- (32) Dietrich, J., Neisig, A., Hou, X. H., Wegener, A. M. K., Gajhede, M., and Geisler, C. (1996) Role of CD3 $\gamma$  in T cell receptor assembly. *J. Cell. Biol.* 132, 299–310.
- (33) Clevers, H., Alarcon, B., Wileman, T., and Terhorst, C. (1988) The T-cell receptor/Cd3 complex—A dynamic protein ensemble. *Annu. Rev. Immunol.* 6, 629–662.
- (34) Szymczak, A. L., Workman, C. J., Wang, Y., Vignali, K. M., Dilioglou, S., Vanin, E. F., and Vignali, D. A. A. (2004) Correction of multi-gene deficiency *in vivo* using a single ‘self-cleaving’ 2A peptide-based retroviral vector (vol 22, pg 589, 2004). *Nat. Biotechnol.* 22, 1590–1590.
- (35) Kuhns, M. S., and Davis, M. M. (2007) Disruption of extracellular interactions impairs T cell receptor-CD3 complex stability and signaling. *Immunity* 26, 357–369.
- (36) Makinen, P. I., Koponen, J. K., Karkkainen, A. M., Malm, T. M., Pulkkinen, K. H., Koistinaho, J., Turunen, M. P., and Yla-Herttuala, S. (2006) Stable RNA interference: Comparison of U6 and H-1 promoters in endothelial cells and in mouse brain. *J. Genet. Med.* 8, 433–441.
- (37) Coin, I., Katritch, V., Sun, T., Xiang, Z., Siu, F. Y., Beyermann, M., Stevens, R. C., and Wang, L. (2013) Genetically encoded chemical probes in cells reveal the binding path of urocortin-I to CRF class B GPCR. *Cell* 155, 1258–1269.
- (38) Grunbeck, A., Huber, T., Abrol, R., Trzaskowski, B., Goddard, W. A., 3rd, and Sakmar, T. P. (2012) Genetically encoded photo-cross-linkers map the binding site of an allosteric drug on a G protein-coupled receptor. *ACS Chem. Biol.* 7, 967–972.
- (39) Geiger, M. W., Elliot, M. M., Karacostas, V. D., Moricone, T. J., Salmon, J. B., Sidel, V. L., and Stonge, M. A. (1984) Aryl azides as protein photolabels—Absorption spectral properties and quantum yields of photodissociation. *Photochem. Photobiol.* 40, 545–548.

(40) Chien, Y. H., Gascoigne, N. R. J., Kavalier, J., Lee, N. E., and Davis, M. M. (1984) Somatic recombination in a murine T-cell receptor gene. *Nature* 309, 322–326.